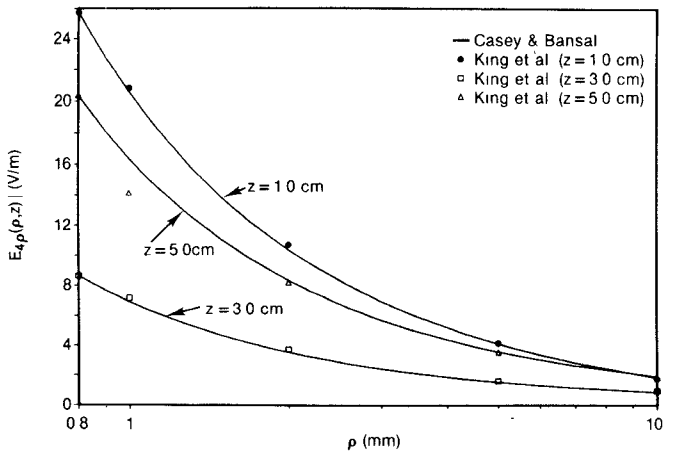

Fig. 6 Magnitude of radial electric field in ambient medium for a full-wave insulated dipole described in Fig. 2 with $h = 6.2$ cm.

conditions as previously mentioned. Note that the same conclusions apply as in the half-wave dipole case.

V. Conclusion

The electric field near an insulted dipole in a dissipative dielectric medium has been calculated by the direct numerical evaluation of a surface integral over the insulation. A comparison of the computed results with those previously obtained by an approximate numerical calculation [1] shows a good agreement for the *radial* component of electric field. It also indicates the limitations of the approximations made in the previous calculation for the computation of the *axial* component of electric field in the vicinity of the insulation.

Appendix

The purpose of this section is to show that $\partial E_z/\partial\rho$ is, in general, discontinuous at $\rho = c$ for the insulated dipole of Fig. 1. For simplicity, assume that only one layer of insulation of outer radius c exists and that the antenna is of infinite length. These assumptions are valid since the original derivation for the current distribution on the finite-length insulated dipole was obtained by taking Fourier transforms (with respect to z) of an infinite-length insulated dipole [2]. From the continuity of H_ϕ at $\rho = c$ [2]:

$$\frac{-j}{\omega}\frac{k_2^2}{\left(k_2^2-\zeta^2\right)}\frac{\partial \bar{E}_{2z}(c,\zeta)}{\partial\rho} = \frac{-j}{\omega}\frac{k_4^2}{\left(k_4^2-\zeta^2\right)}\frac{\partial \bar{E}_{4z}(c,\zeta)}{\partial\rho} \tag{15a}$$

where the bars over the field quantities signify Fourier transforms and ζ is the transform variable. From (15a), we see that $\partial \bar{E}_z/\partial\rho$ is discontinuous at $\rho = c$. From (15a)

$$\frac{\partial \bar{E}_{4z}(c,\zeta)}{\partial\rho} = \left(\frac{k_2}{k_4}\right)^2\frac{\left(k_4^2-\zeta^2\right)}{\left(k_2^2-\zeta^2\right)}\frac{\partial \bar{E}_{2z}(c,\zeta)}{\partial\rho} \tag{15b}$$

Taking the inverse Fourier transform of (15b) yields

$$\frac{\partial E_{4z}(c,z)}{\partial\rho} = \frac{1}{2\pi}\left(\frac{k_2}{k_4}\right)^2 \cdot\int_{-\infty}^{\infty}\frac{\left(k_4^2-\zeta^2\right)}{\left(k_2^2-\zeta^2\right)}\frac{\partial \bar{E}_{2z}(c,\zeta)}{\partial\rho}e^{j\zeta z}d\zeta \neq \frac{\partial E_{2z}(c,z)}{\partial\rho}. \tag{16}$$

References

[1] R. W. P. King, B. S. Trembly, and J. W. Strohbehn, "The electromagnetic field of an insulated antenna in a conducting or dielectric medium," *IEEE Trans Microwave Theory Tech.*, vol. MTT-31, pp. 574–583, July 1983
[2] R. W. P King and G. S. Smith, *Antennas in Matter*. Cambridge, MA: M.I.T. Press, 1981, ch. 8.
[3] S. Silver, *Microwave Antenna Theory and Design*. New York: Dover, 1965, ch. 3.
[4] M. Abramowitz and I A Stegun, *Handbook of Mathematical Functions*, National Bureau of Standards, AMS 55, U.S Dept. of Commerce, Washington, DC, 1964
[5] E. Isaacson and H B. Keller, *Analysis of Numerical Methods*. New York: Wiley, 1966, ch. 7

Measurement Techniques for Planar High-Frequency Circuits

S. E. SCHWARZ AND C. W. TURNER

Abstract — **Planar bismuth bolometers can be used as measuring elements in planar millimeter-wave circuits. These devices are easy to fabricate and calibrate; moreover, their responsivity is thought to be nearly independent of frequency throughout the millimeter-wave regime. Furthermore, they are inherently linear detectors over as much as seven orders of magnitude. Noise-equivalent powers of 2×10^{-10} W/Hz$^{1/2}$ can be attained.**

The high sensitivity of these devices makes them suitable for use in probes. Techniques for measurement of current and reflection coefficient are proposed. Trial measurements, using simulation at 1 GHz, are described.

I. Introduction

Measurements on planar high-frequency circuits are complicated by difficulties that arise in connecting external measuring apparatus to the desired point in the circuit. For instance, a network analyzer cannot give accurate readings unless reflections at its connection to a microcircuit are small and the S-parameters of the connection are precisely known. This is difficult to achieve in practice, especially above 30 GHz. A related problem is that of probing the interior of the circuit, when the measurement is not to be made at one of its ports. Probe measurements in the range 2–18 GHz have been described by Strid and Gleason [1], [2].

One way to minimize the problem of coupling to high-frequency microcircuits is by placing measuring elements on the chip itself. A convenient element for this purpose is the evaporated bismuth microbolometer [3]–[8]. It consists of a small patch of bismuth film, the resistance of which decreases when high-frequency currents pass through it and raise its temperature. The device has several advantages: is is small enough to fit easily anywhere on a microchip; it is very easy to make; and it is a planar element, made with the usual planar techniques. Moreover, it can be highly sensitive. A 4-by-5-μm device was shown to have noise-equivalent power (NEP) of 1.6×10^{-10} W/Hz$^{1/2}$. [3]

In spite of being thermal devices, these bolometers are not necessarily slow: a 4×5-μm device has flat response up to

Manuscript received July 8, 1985; revised November 4, 1985. This work was supported in part by the U.S. National Science Foundation Grant 21488 and the U K. Science and Engineering Research Council

S. E. Schwarz is with the Department of Electrical Engineering, University of California, Berkeley, CA 94720
C. W. Turner is with the Department of Electronic and Electrical Engineering, Kings College London, Strand, London WC2R 2LS, England

IEEE Log Number 8407185.

chopping frequencies beyond 100 kHz. They are also inherently linear and can provide linear measurements over a very wide range. Moreover, they are relatively easy to calibrate. This is because the thickness of the bismuth film (typically less than one micron) is less than the skin depth at all frequencies of interest. For this reason, the impedance of a device much smaller in its lateral dimensions than a wavelength is nearly independent of frequency. This means that the device can be calibrated by observing the change of resistance in response to a chopped sine wave at any convenient audio or radio frequency. Our present observations confirm that constant response extends up to 1 GHz, and from the earlier work [3] it seems probable that that flat response extends to extremely high frequencies, on the order of 2500 GHz. Calibrated in this way, the devices can be used for power measurement. For greatest sensitivity, the bolometer should be connected directly into the microwave circuit, and its resistance should be made equal to the source impedance of the circuit being measured. Alternatively, one can also make measurements without disturbing the circuit under test by making the bolometer resistance much larger than the source impedance. In this case, the bolometers act as high-impedance voltage probes.

A third type of measurement can be made if, instead of building the bolometers directly into the circuit, we use them in external probes that can be moved from place to place. In this case, the measuring probe must be very small, and, hence, it is desirable that the probe itself be made by planar techniques. The microbolometer is well suited for this approach. Its very low NEP makes it possible to space the probe quite far from the circuit being measured; thus, the operation of the circuit will be minimally affected by the probe. Probing techniques will be discussed in Section III.

II. Bolometer Design

For the convenience of the reader, the general properties of our bolometers will be summarized here. More detailed studies of the device will be found elsewhere [6], [8].

The bolometer consists of a bismuth film evaporated between metallic electrodes, as shown in Fig. 1. Bismuth is chosen primarily because of its high resistivity, which gives device resistances in the range 50–300 Ω. A dc current bias is applied and the incident microwave power is chopped. Small changes in the device resistance are produced at the chopping frequency and these combine with the bias current to produce a small voltage across the device at the chopping frequency. The voltage responsibility of the device has a rather modest value, on the order of 10 V/W. When the microwave power supplied to the bolometer is less than about 1 mW, a lock-in amplifier is needed to separate the signal from noise.

Responsivity increases, and NEP and response time decrease, as the lateral dimensions of the bolometer are reduced. Larger devices may, however, be preferred in some applications for ease of fabrication or for making measurements at higher power levels. Thus, it is useful to have some general rules for design. The voltage signal produced by the device, when biased with a constant current, is [3]

$$v = \frac{\alpha V_B W}{G(f) + 2\pi jfC} \tag{1}$$

where V_B is the dc bias voltage, W is the absorbed microwave power, f is the chopping frequency, $G(f)$ is the thermal conductance between the bolometer and its environment, C is the thermal capacity of the bolometer, and α is the temperature coefficient of the resistivity ρ, defined by $\alpha = \rho^{-1}(d\rho/dT)$. The

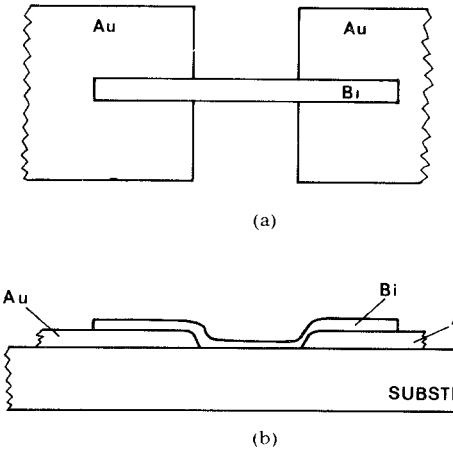

Fig. 1 (a) Top view and (b) sectional view of a typical bolometer. This shape requires little precision in mask alignment.

value of α for evaporated bismuth films was reported [3] to be -3.3×10^{-3}/K; however, this value appears to vary with film thickness [6]. In most cases, $G(f)$ will be dominated by conduction to the substrate. For convenience, we model the bolometer as a hemisphere of radius a, setting the area of the hemisphere $2\pi a^2$ equal to A, the actual area of the bolometer (exclusive of the electrodes). The substrate is assumed to be a semi-infinite solid, and the thermal effect of the electrodes is neglected. In [3], it was shown that in this approximation there is a cutoff frequency $f_{\max}$ given by

$$f_{\max} = \frac{K_s}{AH_s} \tag{2}$$

where K_s is the thermal conductivity of the substrate and H_s is its heat capacity. Responsivity is constant for chopping frequencies less than $f_{\max}$ and decreases as $f^{-1/2}$ immediately above $f_{\max}$. (Above a higher frequency, $f_2 = A^2K_sH_s/2\pi C^2$ responsivity decreases as f^{-1}.) Thus, the chopping frequency should in most cases be made less than $f_{\max}$. The responsivity for $f < f_{\max}$ is [3]

$$R = \frac{v}{W} = \frac{\alpha V_B}{\sqrt{2\pi A\, K_S}}. \tag{3}$$

The experimental performance of three typical devices is described in Table I. Numbers in parentheses are values predicted from (2) and (3) using the following values for the thermal constants [9]: crystal quartz, $K_s = 0.09$ W/cm·deg, $H_s = 1.99$ J/cm^3·deg; glass, $K_s = 0.0085$ W/cm·deg, $H_s = 2$ J/cm^3·deg. Agreement with theory is only within a factor of about two, owing to variations in Bi-film quality and the crudeness of the thermal model. Device 3 is not described by (2) and (3) because its dimensions are large compared with the thickness of the substrate. Devices 1 and 2 have similar responsivity because the larger size of 2 is compensated by the lower thermal conductivity of its substrate. However, device 2 is 1000 times slower than device 1. Moreover, device 2 has considerably poorer NEP than device 1 because of excess noise at its necessarily lower chopping frequencies. (This noise was probably exacerbated by the use of silver paint for making external connections to the device. Thermo-compression bonding should be used instead.) The noise of device 1 was reported to be approximately equal to Johnson noise for chopping frequencies above 250 Hz, even with maximum bias current applied. However, devices 4 and 5 gave lowest NEP at frequencies near $f_{\max}$ because of significant 1/f noise.

TABLE I
EXPERIMENTAL CHARACTERISTICS OF BISMUTH DEVICES

Device	Reference	Resistance, ohms	Device size, length x width	Substrate (thickness)	Bias Voltage (V)	Responsivity (V/W)	NEP ($W/Hz^{\frac{1}{2}}$) (chopping frequency)	f_{max}(Hz)	Burnout Power (mW)
1	Refs. 3,4	170	5μ x 4μ	Crystal Quartz (1 mm)	0.5	10.5 (15)	1.6×10^{-10} (f>250 Hz)	5×10^5 ($2.3.10^5$)	Unknown
2	This work	250	54μ x 60μ	Glass (1 mm)	0.81	9.2 (21)	$2.4.10^{-8}$ (110 Hz)	120(131)	~2
3	This work	250	8.4 mm x 5.0 mm (Note: large compared with substrate thickness)	Glass (1 mm)	0.84	0.026	$2.7.10^{-5}$ (110 Hz)	230	>50
4	Ref. 6	74	4μ x 3.5μ	Glass	0.1	20	5×10^{-10} (1kHz)	3×10^5 (approx.)	
5	Ref. 6	136	4μ x 3.5μ	Air-bridge	0.1	100	1.5×10^{-10} (1kHz)	8×10^4 (approx.)	

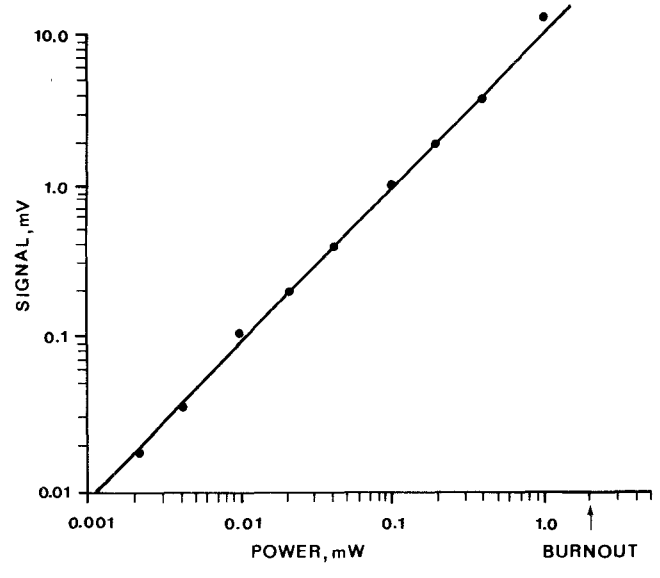

Fig. 2. Signal voltage versus RF power for device 2.

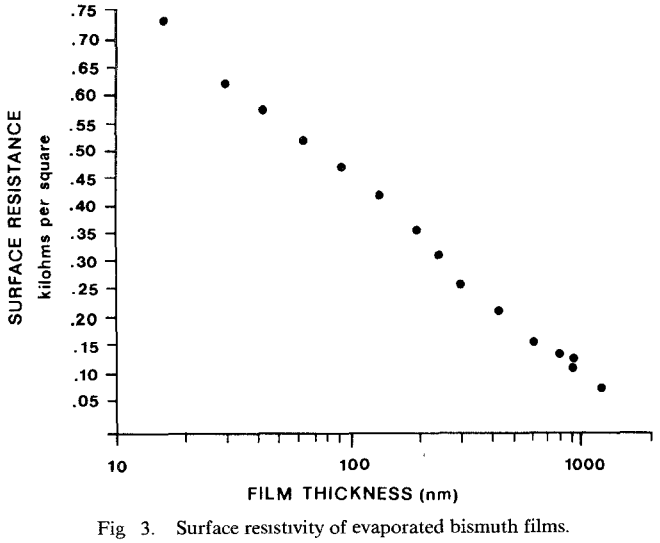

Fig. 3. Surface resistivity of evaporated bismuth films.

Both bias voltage and maximum signal level are limited by the burnout characteristics of the device. Owing to the large thermal conductivity of its substrate, the temperature rise at maximum bias for device 1 was estimated to be about 10° C, and, hence, the failure mechanism was conjectured to be electromigration. For device 2, the temperature rise due to bias was found (by observing the change in dc resistance) to be much larger: a bias of 1.6 V gave a thermal rise of 150°. This is not expected from the simple model, and presumably occurs because of the finite thickness and low thermal conductivity of the substrate. Hence, for device 2, both maximum bias and maximum signal are probably limited by temperature. Unfortunately, burnout ac power was not measured for device 1. However, it may be that electromigration is unimportant for high-frequency ac currents, in which case the burnout power of device 1 might well be larger than that of device 2, even though device 2 is much larger.

One expects that a device of this kind would be linear until signal power creates a sufficiently large rise in temperature to produce a significant change in α. Fig. 2 shows the dependence of output voltage on input signal power for device 2. (These data are obtained using an amplitude-modulated 1-MHz voltage as the input signal. It seems quite unlikely that different results would be obtained at higher signal frequencies.) No significant deviation from linearity is found until signal levels comparable with burnout are reached. This indicates that α is a weak function of temperature. If the maximum signal power of device 1 is comparable with that of 2, as seems likely, it should be linear over seven orders of magnitude.

The bolometers are made as follows. First, the electrode metal is deposited and patterned. The bismuth element is then deposited by evaporation and patterned by liftoff. Surface resistances in the range 75–750 Ω per square are normally obtained. In this range, the surface resistance of the Bi film varies with thickness as shown in Fig. 3. These thickness measurements are from a crystal deposition monitor calibrated with an interference microscope. A mechanical thickness gauge was also used to verify the thickness calibration, with agreement within 10 percent. Nonetheless, remarkably wide variations of surface resistance (over a factor of 10!) are reported in the literature [6], and, in order to produce films with predictable resistivity, it will be necessary to bring the deposition process under more careful control. We note

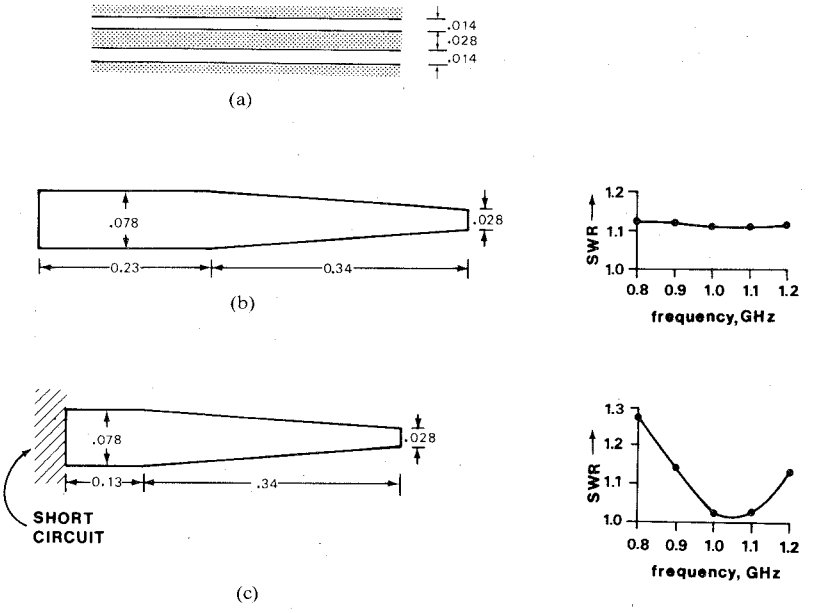

Fig. 4. (a) Dimensions of coplanar waveguide, top view. Shaded area is metal, unshaded area exposed substrate. (b) Broad-band and (c) resonant CPW terminations using 500-Ω/square resistive films. Top views showing dimensions of resistive films to be placed over guide (a). The unit of length is the free-space wavelength.

that surface resistance is not inversely proportional to thickness, except perhaps for the thickest films. The bismuth film must be protected by a film of some insulator, to avoid deterioration caused by atmospheric oxidation.

These same bismuth films should also be useful for constructing resistive devices generally. For large resistors, temperature changes will be small, and surface resistance can be assumed to be constant. Fig. 4 shows a termination for coplanar waveguide. It can be fabricated at any millimeter wavelength by first depositing a thin layer of insulator over the guide and then evaporating and patterning the bismuth film. This termination has been tested in simulation at 1 GHz using 500-Ω/square carbon paper spaced 100 μm above the waveguide. The substrate of the waveguide (shown in Fig. 4(a)) was Emerson and Cuming "Stycast Hi-K" material with relative permittivity of 13 and thickness of 1/4 inch. When the total length is 21 cm, there is no observable transmission of radiation through the attenuator and the reflection is nearly constant at about -25 dB as frequency is varied, as shown in Fig. 4(b) By shortening the load to 14 cm and providing a backshort at its rear end, a resonant load is obtained with reflection of -40 dB at 1 GHz, as shown in Fig. 4(c). These terminations have not been optimized and better results can almost certainly be obtained. The measurements of reflection coefficients were made by using the probes to be described in the following section.

III. Probing Techniques

The low NEP of small planar bismuth bolometers makes it possible to couple them very loosely to the circuit. For example, a bolometer with resistance 100 Z_0, connected across a line of characteristic impedance Z_0, would extract 1 percent of the power from the line and reflect 0.0025 percent, yet for the resulting voltage measurement to be above noise level, a minimum line power of only about 0.02 μW is required. We note that when the bolometer probe is built into a planar circuit, it may be necessary to use capacitors to isolate the bolometer's bias from the microwave circuit.

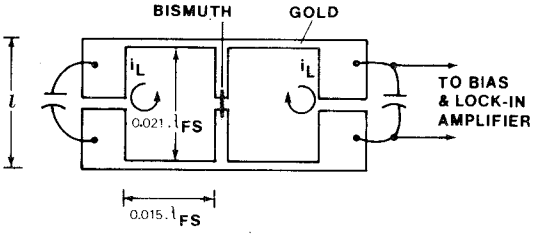

Fig. 5. Planar current probe for coplanar and microstrip lines. λ_{FS} is the free-space wavelength.

In many cases, it is desirable to probe a circuit without making permanent connection to it. This can be done by means of the planar current probe shown in Fig. 5. This particular design is intended for use with the coplanar waveguide of Fig. 4(a), but it should also work with microstrip, since the magnetic field configurations are similar. Planar probes of this sort can be fabricated by conventional lithography on any convenient substrate, and have the advantage that no high-frequency connections need to be brought away from them; only the low-frequency connection to the lock-in amplifier is required. The necessary weak coupling to the circuit is obtained by separating the probe from the circuit with a spacer. In our work, a typical spacing is 0.01 λ_{FS}, where λ_{FS} is the free-space wavelength. The capacitors in Fig. 5 should have reactance less than the bolometer resistance at the operating frequency. For high-frequency work, they can be planar overlap or interdigital capacitors, as convenient. We note that the symmetry of this probe is such that is responds only to the usual "odd" CPW mode. Provided that symmetry is not disturbed, currents associated with the "even" coupled-slotline mode will produce no signal.

The operation of the probe is described as follows. If a current i_L flows in each of the two loops, the voltage induced in series with the waveguide is $v_W = Mj\omega i_L$, where M is the mutual inductance. If Z_L is each loop's series impedance (including twice the bolometer resistance), then $i_L = v_L/Z_L$, where v_L is the voltage around the loop. However, $v_L = -Mj\omega i_W$, where i_W is the current in the waveguide. Hence, the series impedance ap-

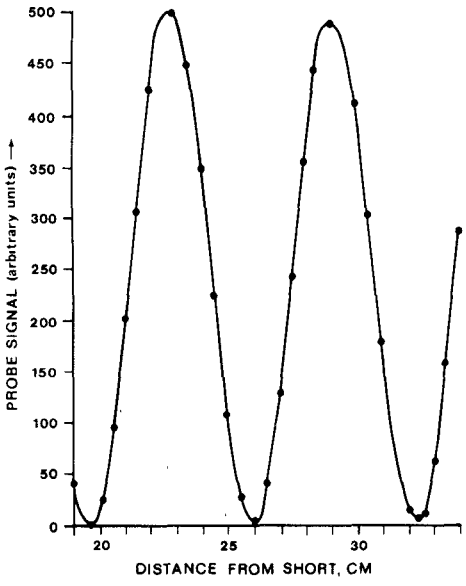

Fig. 6 Measurements with movable current probe on short-circuited coplanar waveguide. Probe signal (proportional to square of RF current) versus position $f = 1$ GHz

pearing in the waveguide because of the probe is

$$Z_W = \frac{v_W}{i_W} = \frac{\omega^2 M^2}{Z_L}. \tag{4}$$

If there were no spacing between the waveguide and the probe, M would be equal to Ll, where L is the waveguide's inductance per unit length and l is the width of the probe. To take account of the spacing s, we write $M = f(s)Ll$, where $f < 1$. Then making use of the property of TEM guide that $L = Z0k/\omega$ (where $k = 2\pi/\lambda_g$, and λ_g is the guide wavelength), we conclude that

$$Z_W = [(kl)f(s)Z_0]^2/Z_L. \tag{5}$$

If Z_W is purely resistive, the fraction of the line power extracted by the probe is approximately Z_W/Z_0.

Using device 2 in the probe of Fig. 5 at 1 GHz, with a spacing of 3 mm, the reflections seen on a network analyzer are less than 1 dB over the entire band 0.1–1.3 GHz. Line powers were measurable down to 3.5 μW, corresponding to a signal of 32 nV at the input of the lock-in amplifier. Using device 1, a much smaller line power, 23 nW would be measurable.

Standing-wave ratio and reflection coefficient can be measured by moving the current probe along the line, very much as one uses a conventional slotted line. Trial measurements were made in this way, using coplanar waveguide at 1 GHz. The probe was moved along a very simple plexiglass track, with no special effort at smoothness or precise alignment with the guide. A typical result, for the case of a shorted line, is shown in Fig. 6. This technique is especially useful for measuring low standing-wave ratios, which are difficult to measure by other means, because they are obscured by reflections at the feed point of the line. Because the bolometer is a square-law detector, small current variations are easily seen, and they can be distinguished from random alignment variations by their periodicity. SWR's as low as 1.02 have been observed.

At higher frequencies, it may be difficult to achieve smooth motion of the probe while maintaining a constant small spacing from the line. However, it seems feasible to fabricate several probes on a single substrate. Using a microscope, the array of probes would then be placed in a stationary position over the waveguide, with suitable spacers used to obtain the desired coupling. With an array density of 10 probes in a half-guide wavelength, it should be possible to determine reflection coefficient with fair accuracy. For the success of this method, it is necessary that the probes be nearly identical. However, the probes are not small, by photolithographic standards, and can be designed in such a way that mask alignment errors have little effect. Thus, the likelihood of achieving the necessary uniformity seems quite high.

ACKNOWLEDGMENT

The authors wish to thank Dr. J. G. Swansom for very useful discussions and assistance. Technical assistance was ably provided by B. Wood and T. Malik.

REFERENCES

[1] E. W. Strid and K. R. Gleason, "A dc-12 GHz monolithic GaAs FET distributed amplifier," *IEEE Trans. Microwave Theory Tech.*, vol. MTT-30, pp 969–75, July 1982.
[2] E. W Strid and K R. Gleason, "Calibration methods for microwave wafer probing," presented at 1984 Int. Microwave Symp., San Francisco, CA, May 30–June 1, 1984.
[3] T. Hwang, S. E. Schwarz, and D. B. Rutledge, "Microbolometers for infrared detection," *Appl Phys. Lett.*, vol. 34, pp. 773–76, June 1, 1979
[4] T Hwang, "Microbolometers for far-infrared detection," Ph.D. thesis, Univ. of California, Berkeley, 1979.
[5] D. P Neikirk and D B. Rutledge, "Air-bridge microbolometer for far-infrared detection," *Appl. Phys Lett.*, vol. 44, pp 153–55, 1984
[6] D. P Neikirk, W. W. Lam, and D. B. Rutledge, "Far-infrared microbolometer detectors," *Int. J. IR MM Waves*, vol. 5, pp. 245–78, Mar. 1984.
[7] D. P. Neikirk and D. B. Rutledge, "Far-infrared embedding impedance measurements," *Int. J. IR MM Waves*, vol. 5, pp. 1017–1026, July 1984.
[8] D. P. Neikirk, "Integrated detector arrays for high-resolution far-infrared imaging," Ph D. thesis, California Inst. of Technol., 1984.
[9] E W Washburn, Ed., *International Critical Tables*, 1st ed. New York: McGraw Hill, 1929, vo 4, pp. 105, 106, 229.

Analysis of Square-Spiral Inductors for Use in MMIC'S

PETER R. SHEPHERD

Abstract—**A method analysis of square spiral inductors for use in monolithic microwave integrated circuits (MMIC's) is presented. The method is based on the coupled microstrip-line theory and incorporates a novel solution to the multicoupled-line problem. The analysis includes the effect of the discontinuities at the right-angled bends in the lines, and also the feedback effect where the lead-out bridge crosses the lines. The method can be used to analyze components with an arbitrary number of spiral turns.**

Theoretical results are compared with the measured S-parameters of a $3\frac{1}{2}$-turn component over the range 2–12 GHz, and reasonable agreement between the two is found.

Manuscript received August 22, 1985; revised November 20, 1985. This work was supported in part by the Procurement Executive (DCVD), U. K. Ministry of Defense

The author is with the Microwave Solid-State Group, Department of Electrical and Electronic Engineering, University of Leeds, Leeds LS2 9JT, U.K.

IEEE Log Number 8407186